ACS Sustainable Chemistry & Engineering

Research Article

pubs.acs.org/journal/ascecg

Green–Silver Nanoparticle-Decorated Multiwalled Carbon Nanotube: A Precursor for Fabrication of Multifunctional Biobased Sustainable Nanocomposites

Sujata Pramanik,[†] Jayanta Hazarika,[‡] Ashok Kumar,[‡] Lipika Aidew,[§] Alak K. Buragohain,[§] and Niranjan Karak*[,†]

[†]Advanced Polymer and Nanomaterial Laboratory, Department of Chemical Sciences, Tezpur University, Tezpur 784028, India

[‡]Material Research Laboratory, Department of Physics, Tezpur University, Tezpur 784028, India

[§]Department of Molecular Biology and Biotechnology, Tezpur University, Tezpur 784028, India

Supporting Information

ABSTRACT: The article highlights the ultrasonication-assisted and diethanol fatty amide of castor oil (DEFA)-mediated bioreduction of silver (Ag) acetate in the presence of multiwalled carbon nanotubes (MWCNT) by a facile and environmentally benign "single-step one-pot approach". DEFA was used to impart a "green capping" attribute to the Ag nanoparticles and noncovalent functionalization of MWCNT. Biobased sustainable hyperbranched poly(ester amide) (HBPEA) nanocomposites were prepared by an *in situ* technique using DEFA-functionalized "Ag nanoparticles-decorated MWCNT" (AgCNT) as one of the starting components. A FTIR spectroscopic tool helped to delve into the probable complexation mechanism of Ag ions with DEFA and their subsequent reduction to Ag nanoparticles. Ag nanoparticles so formed on the surface of the nanotubes in the nanocomposites ranged within a size window of 2–9 nm. X-ray diffractogram indexed for (100), (110), and (111) facets of Ag nanoparticles along with the (002) plane of the nanotubes and the appearance of AgL_β in electron dispersive X-ray spectrum validated the formation of Ag nanoparticles in the nanocomposites. The dose-dependent increment in the performance, particularly the tensile strength (9.5–15.2 MPa), and antibacterial activity against both Gram positive and Gram negative bacterial strains with DEFA-functionalized AgCNT content in the nanocomposites were observed. The significant bactericidal activity, pronounced sheet resistance of 10^6 Ω/sq, mechanical performance, and thermal stability up to 325 °C of the nanocomposites labeled them as potent antibacterial and thermostable antistatic sustainable materials for different advanced applications including coatings, textiles, biomedical electronics, and so on.

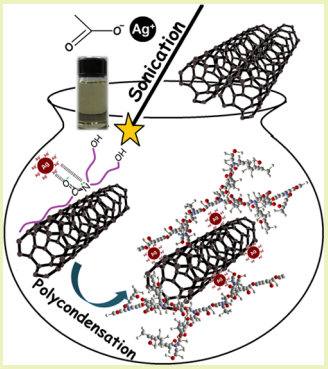

KEYWORDS: *Castor oil, Bioreduction, Biofunctionalization, Antibacterial, Antistatic, Thermostable*

INTRODUCTION

The phenomenal properties of Ag nanoparticles, primarily attributed to their quantum confinement effect, have conferred them a special niche in domains ranging from biomedical to coating industries in the last two decades.[1] Green technology searches for potential bioresources to replace conventional reductive techniques using hydrazine, sodium borohydride, N,N-dimethylformamide, citric acid, and so on for reduction of silver salts.[2] In this regard, Sharma et al.[3] have reviewed the multifunctional role of macromolecules including carbohydrates, starch, and biomolecules including phytochemicals as reducing agents and nanoscale templates for the preparation of Ag nanoparticles. Different microorganisms including bacteria and fungi, as well as irradiation, that aid in the preparation of Ag nanoparticles using metal salt solution have also been documented in contemporary times.[3]

The "contact sport" between zero- and one-dimensional nanomaterials amalgamates the novel properties of both and, thus, continues to carve out endless advances across the globe.[4] Among different one-dimensional nanomaterials, multiwalled carbon nanotubes (MWCNT) have their own advantages, *viz.*, exceptional electrical, mechanical, and thermal properites along with high aspect ratio and low density.[5] Despite possessing such inherent properties, MWCNT *per se* lacks dispersion or interfacial adhesion with the surrounding matrix.[5] Immense efforts are made to functionalize these nanotubes for tailoring their interfacial surface properties without distorting the $\pi-\pi$ structural integrity.[6] Further, it is worth noting that the nanoparticles exhibit remarkable and unique properties when their dimensions are reduced to the order of that of the Fermi wavelength of an electron wherein their properties are dictated by quantum mechanical rules.[7]

The high active surface area of Ag nanoparticles afford better interaction with MWCNT. Gao et al. reported three basic

Received: May 23, 2014
Revised: October 7, 2014
Published: October 15, 2014

   dx.doi.org/10.1021/sc500332t | ACS Sustainable Chem. Eng. 2014, 2, 2510–2518

techniques apart from other physical, chemical, and electrochemical methods for the preparation of MWCNT−Ag nanoparticle nanohybrids.[7] These include "separate", "parasitical", and "simultaneous" methodologies that deal with exohedral *ex situ* and *in situ* and endohedral preparations of the nanohybrids, respectively. Among these three,[7] the *in situ* method seems to be interesting in context of achieving Ag nanoparticles-decorated nanotubes using a biobased sustainable resource. To this end, castor oil seems to be an important candidate amidst all other bioresources owing to its numerous advantages. It is one of the most important nonedible oils used industrially that possesses more than 95% ricinoleic acid, thereby making it comparable to that of any pure chemical.[8] The exploration of a readily available bioresource like castor oil (India being the second largest producer after Brazil) and the use of its fatty amide derivative as a functionalizing agent for MWCNT and for the bioreduction of Ag nanoparticles also add an edge to the above proposition. Moreover, the use of the diethanol fatty amide of castor oil (DEFA) as one of the reactants is expected to provide uniform dispersion and stronger interfacial interactions between MWCNT and Ag nanoparticles under the generated conditions. The subsequent polymerization of DEFA using dibasic acids/anhydrides helps to attain material properties in the resultant polymeric nanocomposites.[9]

This approach of using castor oil as one of the starting materials in the aforementioned task is consistent with the seventh postulate of the 12 green chemistry principles.[10] The biomimetic approach of unlocking the "three-dimensional dendritic" pervasive topologies of nature in the above fabrication of "hyperbranched poly(ester amide)" (HBPEA), amalgamating the properties of both polyesters and polyamides, adds a whole new perspective in the realm of multifaceted materials.[10] The formation of HBPEA using biorenewables guarantees to shift society into a new paradigm to address a cocktail of problems ranging from sustainability to environmental footprints. The combination of castor oil and MWCNT is a contribution toward sustainability in context of functionalization of nanotubes and creating a favorable locale for the bioreduction of Ag ions and decoration of the same onto the nanotubes. Although Ag nanoparticles are a widely acclaimed bacteriocidal agent owing to their antibacterial activity, the rationale behind the use of MWCNT along with Ag nanoparticles is to impart a reinforcing effect[11] and antistatic property[12] of nanotubes in the prepared nanocomposites. The unison of a broad bacteriocidal and antistatic activities and pronounced performance is foreseen for the fabrication of multifunctional nanocomposites. MWCNT can also form prominent network structure via direct nanotube−nanotube interactions and chain bridging interactions with macromolecular DEFA chain holding two nanotubes. These interconnected nanotube structures are envisaged to result in an enhanced mechanical property in the nanocomposites as compared to Ag nanoparticles.[11] In view of present desires, the fabrication of Ag nanoparticles-decorated MWCNT (AgCNT) using DEFA is an important proposition in context of using potential bioresources. Nevertheless, *in situ* preparation of a biobased ternary material, *viz.*, AgCNT/biobased HBPEA nanocomposites in a single pot, has not been reported till date.

In context to the above, the unique properties of AgCNT in the biobased nanocomposites can be explored in high value-added materials used for coatings, textiles, biomedical electronics, and so on. Addressing the formidable problems associated with the aforementioned domains such as microbial and small particulate contaminants and electrostatic charging calls for a cost-effective and potent sustainable technology for use in the design of efficient antistatic and antimicrobial materials in water filters, advanced textile additives, and thin films.[6] In appreciation of the foregoing technologies, the authors report on the fabrication of a AgCNT/castor oil-based HBPEA nanocomposites for application in advanced value-added materials.

Thus, in this work, an attempt is made to use DEFA-functionalized AgCNT as a precursor for *in situ* preparation of biobased HBPEA sustainable nanocomposites. A plausible mechanistic approach for the formation of DEFA-functionalized AgCNT is attempted. Furthermore, the bactericidal activity against a spectrum of bacterial species and their recyclability are scrutinized together with evaluation of the antistatic property of the nanocomposites for forwarding them in their potential advanced applications.

EXPERIMENTAL SECTION

Materials. A batch of MWCNT having purity of around 95 wt % and an average external diameter of ∼10−15 nm was purchased from Hanwha Nanotech Corp., Korea. CH_3COOAg was purchased from Sigma-Aldrich, India, and used as received. The starting materials for the preparation of HBPEA like castor oil (Sigma-Aldrich, India), isophthalic acid (Sisco Research Laboratory Pvt., Ltd., India), phthalic anhydride (Merck, India), and diethanol amine (Merck, India) were used after drying in a vacuum oven at 45−50 °C for 24 h. Maleic anhydride (Merck, Germany) was used post-drying under vacuum at 30 °C. The bisphenol A-based epoxy resin (BPA, Araldite LY 250) (180−190 g/equiv epoxy and 1.16 g/cm^3 density at 25 °C) and poly(amido amine) (HY 840) Hindustan Ciba Geigy, Ltd., Mumbai, were utilized without further purification. The solvents including methanol, benzene, tetrahydrofuran (THF), dimethylacetamide (DMAc), and dimethyl sulfoxide (DMSO) were distilled before use. The bacterial strains such as Gram negative (*Escherichia coli* DH5α and *Klebsiella pneumonia* MTCC618), Gram positive (*Bacillus subtilis* MTCC441 and *Staphylococcus aureus* MTCC373), and acid fast (*Mycobacterium smegmatis* ATCC14468) were obtained from the Department of Molecular Biology and Biotechnology, Tezpur University. All other chemicals used in the present work were of analytical grade and use without any purification.

Preparation of DEFA. DEFA was prepared by a transamidation reaction using transesterified castor oil (using methanol) and diethanol amine (DiEA) in the presence of sodium methxide as the catalyst.[10]

Preparation of DEFA-Functionalized AgCNT. Ag nanoparticles were prepared using CH_3COOAg (in varying wt % of 0.25, 0.5 and 1) as the metal precursor with MWCNT (0.25 wt % with respect to DEFA) as the template and DEFA as the reducing as well as stabilizing agent by an *in situ* reduction technique. The reaction was accomplished with the aid of a sonicator probe, while maintaining the temperature of the ultrasonicating vessel at 4 °C. A control reaction without using Ag salts was also carried out under the same conditions using only nanotubes.

***In Situ* Preparation of Ag Nanoparticles-Decorated MWCNT/HBPEA Nanocomposites.** DEFA-functionalized AgCNT (prepared by varying CH_3COOAg wt % of 0.25, 0.5, and 1 with respect to DEFA) were used as one of the reactive components in the polycondensation reaction with the dibasic acids along with DiEA as the multifunctional moiety. The reaction was carried out in a jacketed vessel using sodium methoxide (0.8 wt % with respect to DEFA) as the catalyst with continuous mechanical stirring under the inert nitrogen atmosphere. The resinification reaction was accomplished in a heating mantle by adjusting the temperature at 150 °C for 0.5 h, 185 °C for a subsequent 1.5 h, and 200−220 °C for 0.25 h. AgCNT/HBPEA nanocomposites prepared with 0.25, 0.5, and 1 wt % of DEFA-functionalized AgCNT separately were encoded as HPAgCNT0.25, HPAgCNT0.5, and HPAgCNT1, respectively. The

prepared nanocomposites were baked using glycidyl ether of bisphenol A epoxy resin (60:40 weight ratio of resin is to epoxy) and poly(amido amine) (50 wt % with respect to epoxy).[10]

Antibacterial Activity. The test bacterial strains were cultured in Mueller Hinton broth media at 37 °C for 18 h and then suspended in an isotonic solution of NaCl (0.85%) to maintain the turbidity of 0.5 as per McFarland standard of the cells (~1 × 10^8 CFU/mL).[13] An amount of 30 μL of the treated bacterial culture was spread in Mueller Hinton agar plates separately and incubated at 37 °C. An aliquot of 100 μL of the nanocomposites (maintaining the concentrations of 0.1 g of nanocomposites per mL of 10% (v/v) DMSO) was incubated with the bacterial culture at 37 °C for 8 h. The bacterial colonies were counted at regular intervals every 2 h. The antibacterial assay was performed using streptomycin sulfate as the positive control, and the results were averaged over a set of three independent experiments. The death rate of the bacteria was calculated using the following eq 1[14]

$$\text{Death rate (\%)} = [(\text{counts in the control}) - (\text{counts upon incubated with the nanocomposites})]/(\text{counts in the control}) \quad (1)$$

Instruments and Testing Methods. FTIR spectra of DEFA-functionalized AgCNT and nanocomposites were performed by Impact 410, Nicolet, U.S.A., using potassium bromide pellets over the wavenumber range of 4000−500 cm^{-1}. The dispersion of DEFA-functionalized AgCNT in the nanocomposite was visualized using JEOL 2100X electron microscope operating at 200 kV voltage. The X-ray diffraction (XRD) study was carried out by a Rigaku X-ray diffractometer (Miniflex, U.K.) equipped with Cu Kα irradiation (λ = 0.154 nm) over a range of 2θ = 10−70° at scanning rate of 2°/min at room temperature. The presence of Ag in the nanocomposites was investigated by electron dispersive X-ray (EDX) JSM-6390LV. Tensile strength and elongation at break of the nanocomposites were measured by the Universal Testing Machine (UTM) of model Jinan WDW 10, China, with a 500 N load cell and at 20 mm/min crosshead speed. The tensile test was carried out as per the standard ASTM D-882 on rectangular-shaped films having dimensions of 6 cm × 1 cm × 0.03 cm. The gloss, scratch hardness, and impact resistance of the cured nanocomposite films were measured as per the standard methods. Thermogravimetric analysis (TGA) was done by a Shimadzu, U.S.A., thermal analyzer, TGA50, at a nitrogen flow rate of 30 mL/min from 25 to 700 °C at the heating rate of 10 °C/min.

The standard four-probe technique with linear configuration was used to measure the sheet resistance of the rectangular-shaped thermosetting HBPEA and nanocomposite films having dimensions of 2 cm × 1 cm. The films were casted onto the glass plates using an adjustable film applicator of Sheen Instruments Incorporation, Ltd., U.K. The four-point probe in the in-line type is shown schematically in Figure S1 of the Supporting Information. The resistivities of the films are given by the following eq 2[15]

$$\rho = \frac{V}{I}\frac{2\pi}{\frac{1}{S1}+\frac{1}{S3}-\frac{1}{(S2+S1)}-\frac{1}{(S2+S3)}} \quad (2)$$

where ρ is the resistivity, V is the potential difference or voltage drop across two probes, I is the current across the other two probes and S1, S2, and S3 are the distance between the four probes in the in-line type arrangement shown in Figure S1 of Supporting Information.

Because S1 = S2 = S3, eq 2 reduces to eq 3

$$\rho = \frac{V}{I}2\pi S \quad (3)$$

As the films are very thin resting on insulating glass plates, eq 3 becomes

$$\frac{\rho}{d} = \frac{V}{I}\frac{\pi}{\ln 2} = 4.532\frac{V}{I} \quad (4)$$

where (ρ/d) is the sheet resistance

Equation 4 is employed for calculating the sheet resistance of the films.

RESULT AND DISCUSSIONS

Plausible Mechanism in Formation of DEFA-Functionalized AgCNT. The adsorption, complexation, and bioreduction of Ag salt and noncovalent functionalization of the nanotubes were exploited using the same template of DEFA in a single pot without using any external reducing or stabilizing agent. The rationale behind the choice of DEFA relies on the fact that it possesses both reducing and templating attributes for the *in situ* preparation of DEFA-functionalized AgCNT. DEFA adsorbed onto Ag salt (owing to secondary electrostatic interactions)[16] formed nanoscopic domains/nanocavities with hydrophobic interiors that helped adherence with the nanotubes. In other words, the presence of a suitable microenvironment of DEFA facilitated both complexation of Ag salt and noncovalent functionalization of the nanotubes. The long hydrocarbon chain and amide functional groups of DEFA formed reactive sites for the surface functionalization of the nanotubes and reduction of Ag salt, respectively.[16] The −OH groups of the same conferred steric stabilization to the nanomaterials against aggregation. Such individual interactions are weak, but the integral interactions resulted in high adsorption forces. Further, the bioreduction of Ag acetate using DEFA is based on supramolecular complexation of Ag ions with an amide group[17] of DEFA that acts as an interacting ligand with lone pair on the N atom as a hard base. In light of the hard−soft acid base (HSAB) principle, a competition occurs between the two, *viz.,* N atom of DEFA (hard base), which is stronger than the acetate ion (soft base) sets up, wherein the former replaces the latter and effectively coordinates with Ag ions. The accessibility of the lone pair of tertiary N atoms of DEFA renders stability to the Ag ions through electrostatic attractions between the two. Moreover, the coordination of the carbonyl amide O atom with Ag ions[18] by an electron-transfer mechanism (as supported by FTIR study) results in alternate capping of Ag nanoparticles. A similar study by Zamiri et al.[18] validated the stabilizing mechanism of Ag nanoparticles by an O atom of the carbonyl amide. In essence, the encapsulation by DEFA creates a diffusion barrier to the growing Ag nuclei and predominantly stabilizes Ag nanoparticles by electrostatic interaction.[19] Further, the hydrophobic C-18 alkyl chain of DEFA adheres onto the nanotubes via CH−π interactions[6] and provides a locale for Ag nanoparticles to anchor onto its surface using the amide group attached with the hydrocarbon chain as a linker. This was supported by one of such representative works reported by Zamudio and his co-workers,[20] with Ag nanoparticles (having diameter 2−10 nm) anchored onto N-doped MWCNT. This method involves covalent functionalization of the nanotubes using a plasma technique, which is cumbersome, costly, and requires special equipment and creation of a vacuum. Further, the covalent functionalization results in corrugated structure in N-doped nanotubes, which may lead to deterioration of the properties. The reported method in our work involves noncovalent functionalization of the nanotubes. The green chemistry tool of sonication is exploited in our work to form and anchor Ag nanoparticles onto the surface of the nanotubes using a sustainable bioresource.

In addition to the above interactions, the comprehending role of ultrasonication is indispensable in the context of preparation of DEFA-functionalized AgCNT. The implosion of

Scheme 1. Plausible Mechanism of Formation of DEFA−AgCNT and Its Polymerization To Yield Nanocomposites

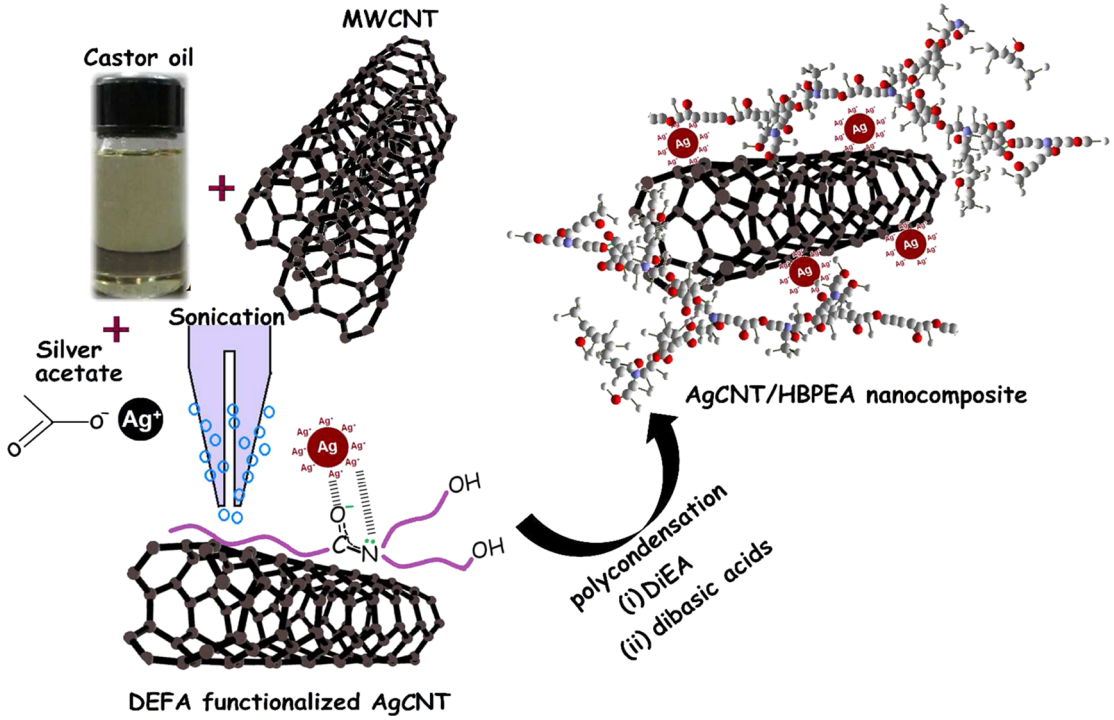

small cavitation bubbles and dissipation of energy by microstreaming during compression and rarefaction acoustic cycles of sonication are also instrumental in driving both the reduction of Ag salts and exfoliation of the nanotubes.[6]

Preparation of Biobased AgCNT/HBPEA Nanocomposites. DEFA-functionalized AgCNT was used as a precursor for an *in situ* surface-initiated polycondensation reaction with the dibasic acids and DiEA to prepare HBPEA. The nanotubes functionalized with DEFA possessing high esterification rates toward the dibasic acids served as the difunctional monomers along with DiEA as the multifunctional building block to form HBPEA.[10] DEFA also acted as a reactive diluent to aid in the degree of dispersion of the nanotubes in the polymeric matrix. The formation of polymeric chains impeded the Brownian motion of the nanomaterials and thereby aided their stabilization. The narrow size window of the Ag nanoparticles and good dispersion of the same in HBPEA matrix (evident from HRTEM study) are primarily attributed to steric stabilization.[18] The decrease in the entropy or possible orientations of HBPEA chains adsorbed onto AgCNT resulted in a volume restriction, and the osmotic effect due to the high concentration of the polymeric chains in between the two AgCNT forms the basis of the steric stabilization process.[6] In other words, the architectural features of HBPEA served as nanocavities with ligand sites for stabilization and preorganization of AgCNT, which was validated using the FTIR tool. Scheme 1 presents the preparative protocol of the DEFA-functionalized AgCNT/HBPEA nanocomposite.

Structural Characterization. *UV−Visible Study.* The UV−vis spectra of DEFA-functionalized AgCNT (containing 0.25% Ag), DEFA-functionalized nanotubes, and HPAgCNT1 are shown in Figure 1. The UV−vis absorption band of the nanohybrid contained the characteristic 1D van Hove singularities of the nanotubes at around 264 nm. The absence of the plasmon absorption of Ag nanoparticles is attributed to its quantum size effect. This observation is consistent with the

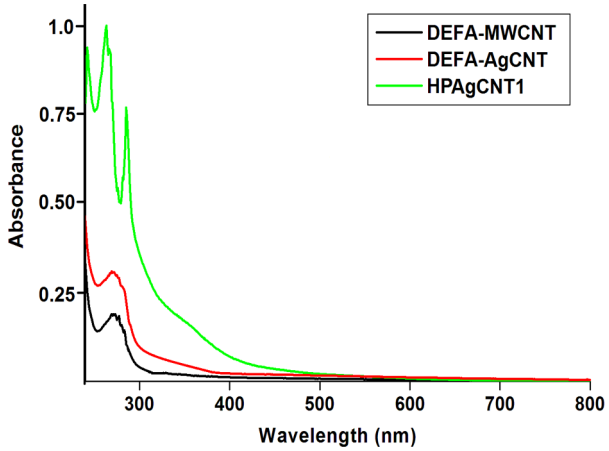

Figure 1. UV−vis spectra of DEFA-functionalized MWCNT, DEFA-functionalized AgCNT, and HPAgCNT1.

reports of Zheng et al.[21] according to which metal nanoparticles with diameter less than 10 nm including nanoclusters are too small to possess the continuous density of states to support the plasmon characteristics of comparatively larger metal nanoparticles. This was further supported by the recent report by Brumbaugh and his co-workers, which documented that the UV−vis spectral feature of "ultrasmall nanoparticles" is a function of their size.[22] The appearance of the absorption band at around 283 nm is attributed to the formation of a carbonyl ester group in the backbone of HBPEA.

FTIR Study. FTIR spectra of DEFA-functionalized AgCNT (containing 0.25% Ag) (both immediately after mixing and after sonication), HPAgCNT0.25, HPAgCNT0.5, and HPAgCNT1 are shown in Figure 2. Attempts were made to ascertain the formation of the above-mentioned coordination complex of Ag salt with DEFA using FTIR. The carbonyl amide stretching and −CH═CH− bending vibrations of DEFA

dx.doi.org/10.1021/sc500332t | ACS Sustainable Chem. Eng. 2014, 2, 2510−2518

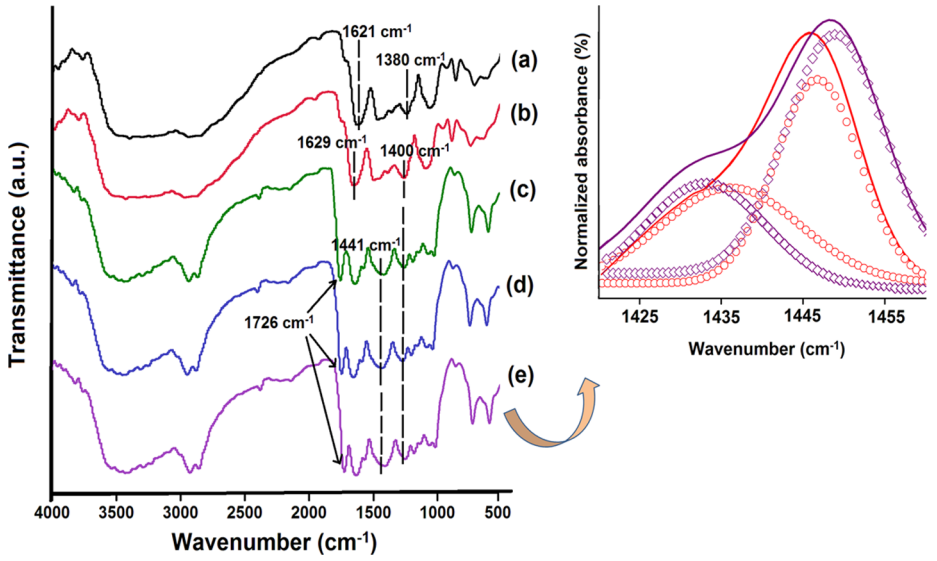

Figure 2. FTIR spectra of (a) DEFA-functionalized AgCNT (containing 0.25% Ag) immediately after mixing, (b) DEFA-functionalized AgCNT (containing 0.25% Ag) after sonication, (c) HPAgCNT0.25, (d) HPAgCNT0.5, and (e) HPAgCNT1 with the inset of the deconvoluted CH peaks of DEFA-functionalized AgCNT and HPAgCNT1.

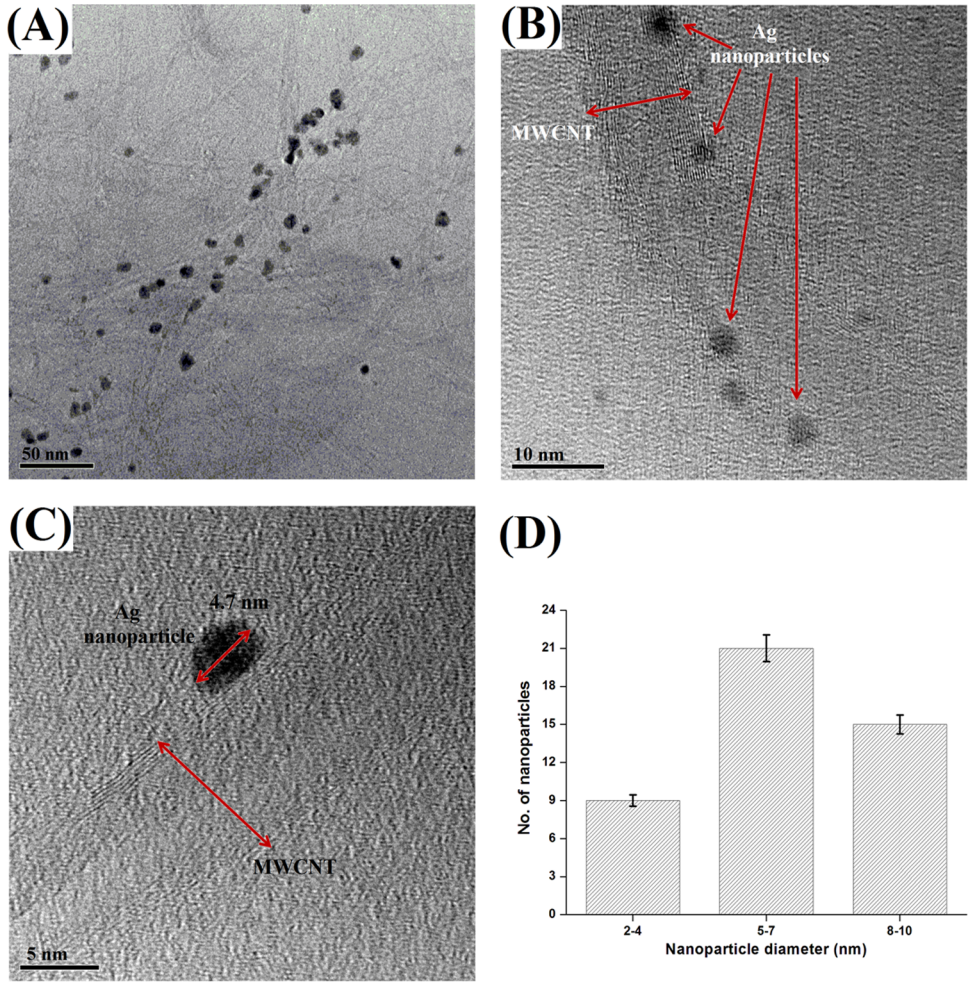

Figure 3. (A), (B), (C) HRTEM micrographs of HPAgCNT1 at magnification scales of 50, 10, and 5 nm, respectively. (D) Particle size histogram.

appeared at around 1621 and 772 cm^{-1}, respectively.[10] The FTIR spectra of DEFA immediately after mixing the Ag salt and the nanotubes showed shifting in the C═O carbonyl amide and C−N bond vibrations. The absorption peak centered at 1621 and 1380 cm^{-1}, fundamental to the stretching vibrations of the carbonyl amide ester and C−N bond of DEFA, shifted to

dx.doi.org/10.1021/sc500332t | ACS Sustainable Chem. Eng. 2014, 2, 2510−2518

1629 and 1400 cm^{-1}, respectively, owing to the interaction of Ag ions and the nanotubes with DEFA. The coordination of the Ag ion with the ester and N atom lone pair of the carbonyl amide functional group resulted in the shifting of their bond vibrations.[19] However, upon sonication (formation of Ag^0 nanoparticles), DEFA-functionalized AgCNT showed that the carbonyl amide bond vibrations resorted back to their original wavenumber (same as DEFA), but C−N bond vibration remained at 1400 cm^{-1}. This observation justified the formation of a coordination complex of Ag salt using both the O atom and N atom of the carbonyl amide bond of DEFA, with subsequent stabilization of Ag nanoparticles so formed by association with the N atom of the same. Unlike other reported protocols wherein hydroxyl groups take part in the reduction process, the carbonyl amide is the key player in the bioreduction of the Ag salt in this present work. This assumption is supported by the absorption peak of −OH, which remains intact without shifting (in the case of DEFA and DEFA-functionalized AgCNT). Further, the appearance of the absorption band at around 1726 cm^{-1} confirmed the formation of the ester groups in the backbone of HBPEA.[10] The CH bending peak of HBPEA appears at 1441 cm^{-1}.[10] The interaction of the nanotubes with long fatty acid chains was attested by the broadening of the CH bending bands of the nanocomposites with respect to DEFA-functionalized AgCNT.[6] The splitting of the CH peak of HPAgCNT1 into a doublet upon deconvolution justified the aforestated interaction of the nanomaterials with the polymer matrix (Figure 2, inset).

HRTEM Study. The HRTEM micrograph of HPAgCNT1 at the scale bar of 50 nm (Figure 3a) shows the preferential distribution of Ag nanoparticles onto the surface of the nanotubes dispersed in the polymer matrix. Figure 3b shows the close proximity of the adsorption of Ag nanoparticles on the surface of the nanotubes. Such nonuniform distribution of Ag nanoparticles in the nanocomposite may be attributed to the high active surface area and surface energy of the nanotubes and the formation of dangling bonds on the surface of the nanotubes during sonication,[6] which creates adsorption sites for the growing Ag nanoparticles. The interface between the Ag nanoparticle and the surface of the nanotube (Figure 3c) was indicative of the fact that Ag nanoparticles used the nanotube surface as a template for their growth. It was apparent from the particle size histograms of the nanocomposites (Figure 3a), deduced using Fiji software, that Ag nanoparticles within the control size range of 2−10 nm remained well dispersed in the polymeric matrix (Figure 3d). It is noteworthy that the highest fraction of Ag nanoparticles lies in the diameter range of 5−7 nm. Further, the disentanglement and well dispersion of the nanotubes reflected from the HRTEM micrograph is supportive of the noncovalent functionalization of the same. The formation of Ag nanoparticles below and above the plane of the nanotubes is shown in Figure S2 of the Supporting Information.

XRD Study. Figure 4 shows X-ray diffractograms of HPAgCNT0.25, HPAgCNT0.5, and HPAgCNT1. While the characteristic (002) Bragg's peak of pristine nanotubes appears at around 26.2°,[6] the peaks centered at around 38°, 44.5°, and 64.5° signifies the (111), (200), and (220) planes of fcc structured Ag nanoparticles, respectively.[2] HBPEA exhibits a broad halo (at around 20°) owing to its amorphousness.[6] The appearance of XRD peaks at around 26°, 38.2°, 44°, and 64.3° in the nanocomposites is ascribed to the presence of the nanotubes and Ag nanoparticles in HBPEA matrix. However,

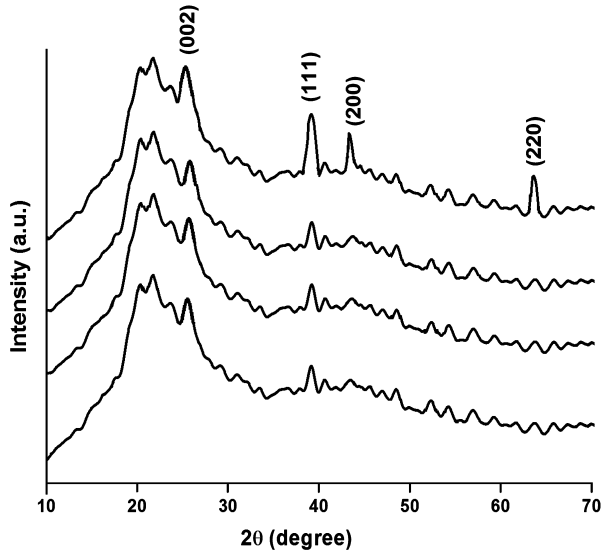

Figure 4. XRD patterns of (a) DEFA−AgCNT, (b) HPAgCNT0.25, (c) HPAgCNT0.5, and (d) HPAgCNT1.

the low intensity of the above-mentioned peaks of the nanocomposites is due to their low content as compared to the polymeric matrix (maximum 1 wt %).

EDX-SEM Study. EDX and corresponding SEM micrographs of HPAgCNT0.25, HPAgCNT0.5, and HPAgCNT1 are shown in Figures 5, 6, and 7, respectively. In contrast to the SEM micrograph of pristine HBPEA[10] exhibiting homogeneous morphology with no segregation, the presence of the nanomaterials is clearly evident from the cross-sectional micrographs of the nanocomposites (Figures 5a, 6a, 7a). The SEM micrographs of the fractured surface of the nanocomposites present an insight into the dispersion scenario of the nanomaterials in the polymeric matrix. As the nanotubes are good electrical conductors, the secondary electrons being generated in SEM micrographs will be comparatively less, resulting in dark regions in the nanocomposites. The micrographs exhibit interconnected fiber-like structures with a polymer matrix surrounding the same, which enhances the compatibility and interfacial interactions between the two. Ag nanoparticles cannot be seen in the SEM micrographs; however, the presence of the same is evident from the HRTEM micrographs.

The EDX spectrum of the nanocomposites (Figures 5b, 6b, 7b) confirm the presence of elemental Ag in the same. The peaks observed at 0.25, 0.39, 0.52, and 3.2 keV are attributed to the binding energies of carbon (CK_α), nitrogen (NK_α), oxygen (OK_α), and silver (AgL_β) respectively.[23] The peak intensity of AgL_β increased with AgCNT content in the nanocomposites, which is evident from the inset tables in Figures 5b, 6b, and 7b.

Performance Study. The epoxy-poly(amido amine)-cured thermosetting DEFA-functionalized AgCNT/HBPEA nanocomposites exhibited pronounced increments in their performance as compared to pristine HBPEA (Table 1). The curing time of the nanocomposites (cured at 150 °C) effectively decreased with an increase in AgCNT content. This is attributed to the presence of AgCNT, which aids in the cross-linking reaction by acting as a pseudo-organometallic catalyst. In other words, the vacant orbitals of Ag and defect sites of the nanotubes of AgCNT are envisaged to coordinate with the lone pair of the O atom of the oxirane ring of epoxy and N atom of HBPEA and poly(amido amine) and thereby aid

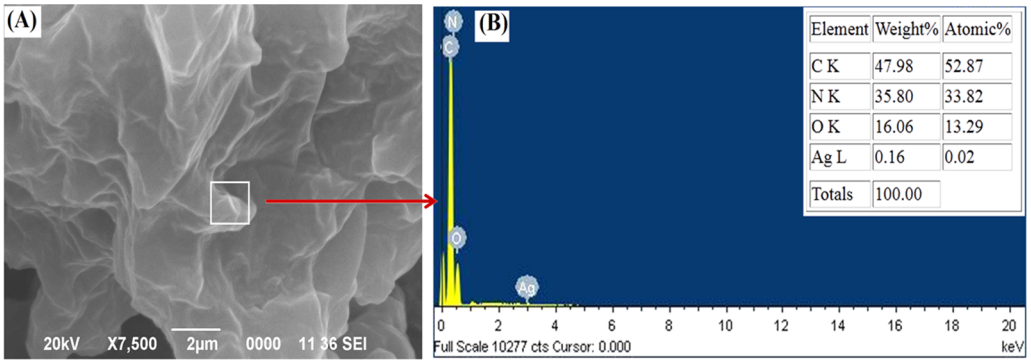

Figure 5. EDX spectrum and SEM micrograph of HPAgCNT0.25.

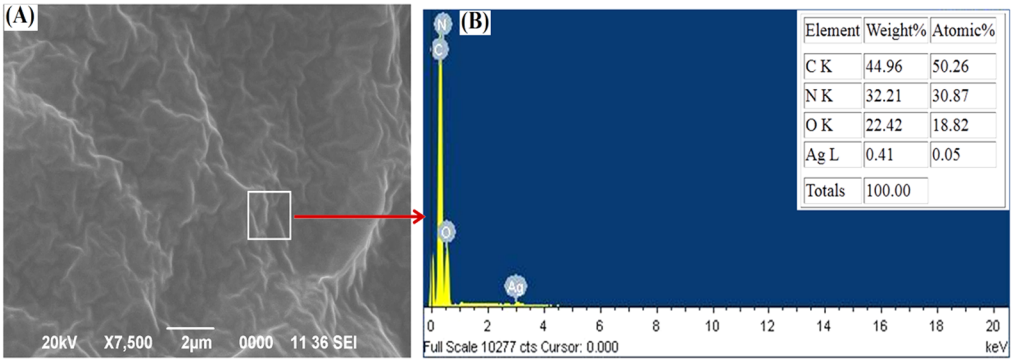

Figure 6. EDX spectrum and SEM micrograph of HPAgCNT0.5.

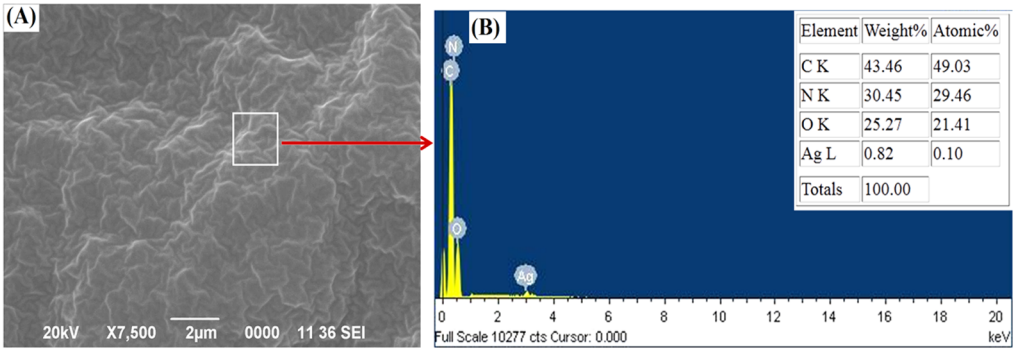

Figure 7. EDX spectrum and SEM micrograph of HPAgCNT1.

Table 1. Performance of DEFA-Functionalized AgCNT/HBPEA Nanocomposite Films

physicomechanical property	HPAgCNT0.25	HPAgCNT0.5	HPAgCNT1
curing time (h)	2.9 ± 0.01	2.6 ± 0.01	2 ± 0.01
gel fraction (%)	77.4 ± 0.2	76.6 ± 0.4	76.1 ± 0.1
scratch hardness (kg)	9.5 ± 0.3	10	10
impact resistance (cm)[a]	>100	>100	>100
gloss at 60°	92.3 ± 0.4	93.7 ± 0.5	94.2 ± 0.5
TS (MPa)	9.5 ± 0.3	11.7 ± 0.2	15.2 ± 0.4
EB (%)	84.3 ± 0.6	83.4 ± 0.5	80.7 ± 0.6

[a]Limit of the instrument is 100 cm.

in bringing the components in close proximity, which facilitates the cross-linking reaction.[24] The cross-linking of HBPEA and its nanocomposites with 0.25 wt % MWCNT and 1 wt % Ag nanoparticles, separately under the curing conditions, took 10, 3.2, and 3 h, respectively. The curing times of the nanocomposites were comparatively lesser than pristine polymer[10] or its nanocomposites using 0.25 wt % MWCNT and 1 wt % Ag nanoparticles, separately (Table 1). Thus, AgCNT forms the key player in the curing process of the nanocomposites by synergistically combining the attributes of both Ag nanoparticles and the nanotubes.

The gloss and scratch hardness increased with AgCNT content in the nanocomposites. The obtained findings are in accord with the presence of profound interfacial interactions of AgCNT with the HBPEA matrix (as evident from FTIR study), which are instrumental in imparting significant dimensional stability and surface texture to the cured thermosetting nanocomposites. The rigidity in the structure (optimum gel fraction) along with the flexibility of the fatty acid chains account for their high impact resistance. The compatibility, interfacial interactions, and nanoreinforcement effect of AgCNT with the polymeric matrix resulted in an increase in the tensile strength of the nanocomposites from 9.5 to 15.2

MPa. The decrement in the elongation at break (EB) is attributed to the restriction in the movement of the polymeric chains owing to their interfacial interaction with AgCNT.[6]

Thermal Study. It is observed from Figure 8 that the inclusion of DEFA-functionalized AgCNT in the preparation of

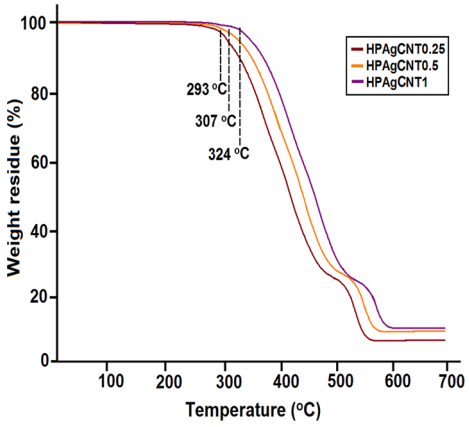

Figure 8. TG thermograms of DEFA-functionalized AgCNT/HBPEA nanocomposites.

HBPEA nanocomposites imparted a dose-dependent thermostability to the system. HBPEA exhibits a two-step degradation owing to the degradation of ester and amide functional groups at 277 and 521 °C, respectively.[10] The increment of AgCNT content from 0.25 to 1 wt % in the nanocomposites increased the thermal stability from 293 to 324 °C. The interfacial interactions of AgCNT with the HBPEA matrix (as evident from FTIR study) and the catalytic role of AgCNT in the cross-linking process of the nanocomposites with epoxy and poly(amido amine) by behaving as a pseudo-organometallic catalyst account for the above findings. Further, the restriction in the movement of HBPEA chains owing to the presence of AgCNT resulted in the improvement of the thermostability of the nanocomposites as compared to the pristine HBPEA.

Antistatic Property. Figure 9 represents the variation of the sheet resistance values of DEFA-functionalized AgCNT and the nanocomposites. DEFA-functionalized AgCNT was found to exhibit sheet resistance of the order of 10^4 to 10^5. HBPEA exhibits sheet resistance of the order of 10^7, which dropped to the order of 10^6 upon incorporation of 0.25 wt % nanotubes in the HBPEA matrix.[6] However, the incorporation of 1 wt % AgCNT decreased the sheet resistance to the order of 10^5 owing to efficient dissipation of the static electric charges. This sheet resistance value is found to be adequate for many applications as mentioned above.

Antibacterial Activity. It was observed from the enumeration of the bacterial death rate (Figure 10) that AgCNT/HBPEA nanocomposites exhibited potent antibacterial activity against acid fast, Gram positive, and Gram negative bacterial strains as compared to the experimental control. These observations are in contrast to our earlier findings wherein pristine HBPEA and the nanocomposite of the same using 0.25 wt % of pristine nanotubes showed selective antibacterial activity against Gram positive bacterial species.[6] The rationale behind the use of a number of bacterial strains is to probe into the broad spectrum antibacterial efficacy of the nanocomposites against the same. So, the bacteria used are the model bacteria for Gram positive, Gram negative, and acid fast bacterial strains, which generally affect such polymeric materials. The incorporation of Ag nanoparticles thus plays a paramount role in widening the antibacterial attributes of DEFA-functionalized AgCNT/HBPEA nanocomposites against a broad spectrum of bacterial species. The electrostatic interactions between Ag and the negative charges of bacterial lipopolysaccharides (key component of outer membrane of Gram negative bacteria) subsequently led to their cellular distortion by different mechanisms (including denaturation of DNA and RNA, generation of reactive oxygen species, and so on) and loss of bacterial replication and viability.[25] Thus, the high surface activity of Ag nanoparticles and MWCNT entities is imperative for imparting significant antibacterial activity.

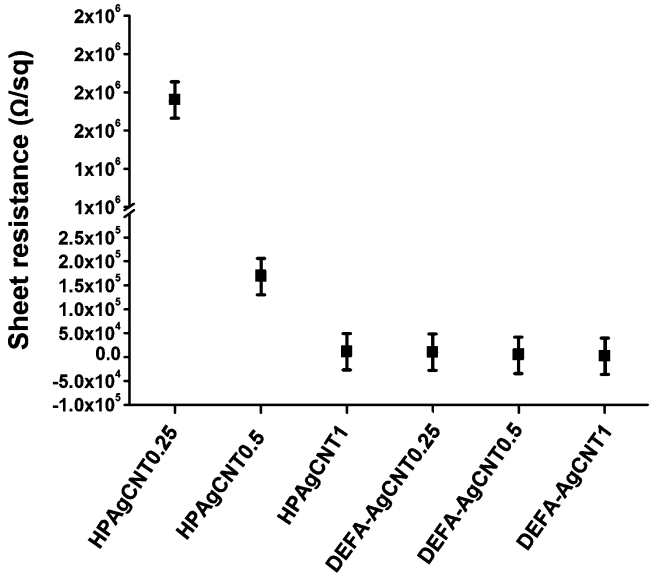

Figure 9. Sheet resistance of DEFA-functionalized AgCNT and its nanocomposites.

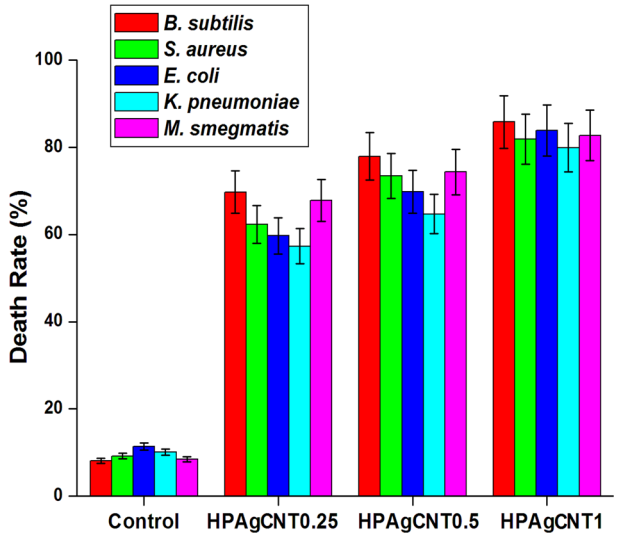

Figure 10. Death rate of bacterial strains upon incubation with DEFA-functionalized AgCNT/HBPEA nanocomposites.

CONCLUSION

The above findings demonstrated a facile one-pot DEFA-functionalized AgCNT preparation without using any solvent or stabilizing agent. Exploiting the concomitant use of green tools of sonication and bioresource, reactive sites of the

dx.doi.org/10.1021/sc500332t | ACS Sustainable Chem. Eng. 2014, 2, 2510−2518

nanotubes are generated for anchoring of Ag nanoparticles and adsorption of DEFA at a shorter reaction time period of 15 min. FTIR, UV−vis, EDX, and HRTEM tools coupled with thermogravimetric analyses support the formation of the DEFA-functionalized AgCNT/HBPEA nanocomposites. Coalescing the multifaceted attributes of the prepared nanocomposites such as antistatic, thermostable, and wider antibacterial properties open new opportunities for advanced sustainable applications in the realm of textiles, biomedical electronics, and coatings.

■ ASSOCIATED CONTENT

Supporting Information

Schematic diagram for the measurement of sheet resistance using four-point probe in the in-line type (Figure S1). HRTEM micrographs of DEFA-functionalized HPAgCNT1 with Ag nanoparticles anchored below and above the plane of the nanotubes (Figure S2). This material is available free of charge via the Internet at http://pubs.acs.org.

■ AUTHOR INFORMATION

Corresponding Author

*E-mail: karakniranjan@yahoo.com. Tel: +91 3712-267327. Fax: +91 3712-267006.

Present Address

A. K. Buragohain: Dibrugarh University, Dibrugarh 786004, India

Notes

The authors declare no competing financial interest.

■ ACKNOWLEDGMENTS

The authors express their gratitude to SAP (UGC), India, for Grant F.3-30/2009(SAP-II) and FIST program-2009 (DST), India, for Grant SR/FST/CSI-203/209/1 dated June 5, 2010. The research is funded by Defense Research Laboratory (DRL), India, through the Grant DRL/1047/TC dated March 2, 2011. RSIC, NEHU, Shillong is gratefully acknowledged for the TEM imaging. The authors also thank Mr. R. Boruah for his help in EDX study.

■ REFERENCES

(1) Satyavani, K.; Gurudeenban, S.; Ramanathan, T.; Balasubramanian, T. Biomedical potential of silver nanoparticles synthesized from calli cells of *Citrullus colocynthis* (L.) schrad. *J. Nanobiotechnol.* **2011**, *9*, 43.

(2) Barua, S.; Konwarh, R.; Bhattacharya, S. S.; Das, P.; Devi, K. S. P.; Maiti, T. K.; Mandal, M.; Karak, N. Non-hazardous anticancerous and antibacterial colloidal 'green' silver nanoparticles. *Colloids Surf., B* **2013**, *105*, 37−42.

(3) Sharma, V. K.; Yngard, R. A.; Lin, Y. Silver nanoparticles: Green synthesis and their antimicrobial activities. *Adv. Colloid Interface Sci.* **2009**, *145* (1−2), 83−96.

(4) Xin, F.; Li, L. Decoration of carbon nanotubes with silver nanoparticles for advanced CNT/polymer nanocomposites. *Composites, Part A* **2011**, *42* (8), 961−967.

(5) Dyke, C. A.; Tour, J. M. Covalent functionalization of single-walled carbon nanotubes for materials applications. *J. Phys. Chem. A* **2004**, *108* (51), 11151−11159.

(6) Pramanik, S.; Barua, N.; Buragohain, A. K.; Hazarika, J.; Kumar, A.; Karak, N. Biofunctionalized multiwalled carbon nanotube: A reactive component for the in situ polymerization of hyperbranched poly (ester amide) and its biophysico interfacial properties. *J. Phys. Chem. C* **2013**, *117* (47), 25097−25107.

(7) Lindberg, V.; Hellsing, B. Metallic quantum dots. *J. Phys.: Condens. Matter* **2005**, *17* (13), S1075−S1094.

(8) Ogunniyi, D. S. Castor oil: a vital industrial raw material. *Bioresour. Technol.* **2006**, *97* (9), 1086−1091.

(9) Anastas, P.; Eghbali, N. Green chemistry: principles and practice. *Chem. Soc. Rev.* **2010**, *39* (1), 301−312.

(10) Pramanik, S.; Konwarh, R.; Sagar, K.; Konwar, B. K.; Karak, N. Bio-degradable vegetable oil based hyperbranched poly (ester amide) as an advanced surface coating material. *Prog. Org. Coat.* **2013**, *76* (4), 689−697.

(11) Wan, H.; Delale, F.; Shen, L. Effect of CNT length and CNT-matrix interphase in carbon nanotube (CNT) reinforced composites. *Mech. Res. Commun.* **2005**, *32* (5), 481−489.

(12) Sangermano, M.; Pegel, S.; Pötschke, P.; Voit, B. Antistatic epoxy coatings with carbon nanotubes obtained by cationic photopolymerization. *Macromol. Rapid Commun.* **2008**, *29* (5), 396−400.

(13) Gao, C.; Yan, D. Hyperbranched polymers: From synthesis to applications. *Prog. Polym. Sci.* **2004**, *29* (3), 183−275.

(14) Liu, S.; Wei, L.; Hao, L.; Fang, N.; Chang, M. W.; Xu, R.; Yang, Y.; Chen, Y. Sharper and faster "nano darts" kill more bacteria: A study of antibacterial activity of individually dispersed pristine single-walled carbon nanotube. *ACS Nano* **2009**, *3* (12), 3891−3902.

(15) Maissel, L. I.; Glang, R. *Handbook of Thin Film Technology*; McGraw-Hill: New York, 1970.

(16) Kang, S. W.; Kim, J. H.; Ko, D.; Kim, C. K.; Won, J.; Char, K.; Kang, Y. S. Complexation of phthalate oxygens in poly(ethylene phthalate) with silver ions and its effect on the formation of silver nanoparticles. *J. Polym. Sci., Part B: Polym. Phys.* **2004**, *42* (18), 3344−3350.

(17) Hakimi, M.; Moeini, K.; Mardani, Z.; Khorrami, F. Crystal structure and characterization of a new eight coordinated cadmium complex. *J. Korean Chem. Soc.* **2013**, *57* (3), 352.

(18) Zamiri, R.; Zakaria, A.; Ahangar, H. A.; Sadrolhosseini, A. R.; Mahdi, M. A. Fabrication of silver nanoparticles dispersed in palm oil using laser ablation. *Int. J. Mol. Sci.* **2010**, *11* (11), 4764−4770.

(19) Qiu, L.; Liu, F.; Zhao, L.; Yang, W.; Yao, J. Evidence of a unique electron donor−acceptor property for platinum nanoparticles as studied by XPS. *Langmuir* **2006**, *22* (10), 4480−4482.

(20) Zamudio, A.; Elías, A. L.; Rodríguez-Manzo, J. A.; López-Urías, F.; Rodríguez-Gattorno, G.; Lupo, F.; Rühle, M.; Smith, D. J.; Terrones, H.; Díaz, D.; Terrones, M. Efficient anchoring of silver nanoparticles on N-doped carbon nanotubes. *Small* **2006**, *2* (3), 346−350.

(21) Zheng, J.; Zhang, C.; Dickson, R. M. Highly fluorescent, water-soluble, size-tunable gold quantum dots. *Phys. Rev. Lett.* **2004**, *93* (7), 077402(1−4).

(22) Brumbaugh, A. D.; Cohen, K. A.; Angelo, S. K. Ultrasmall copper nanoparticles synthesized with a plant tea reducing agent. *ACS Sustainable Chem. Eng.* **2014**, *2* (8), 1933−1939.

(23) Khan, M. A. M.; Kumar, S.; Ahamed, M.; Alrokayan, S. A.; AlSalhi, M. S. Structural and thermal studies of silver nanoparticles and electrical transport study of their thin films. *Nanoscale Res. Lett.* **2011**, *6* (1), 434.

(24) Dong, Y. B.; Geng, Y.; Ma, J. P.; Huang, R. Q. Organometallic silver (I) coordination polymers and supramolecular complexes based on novel multidentate thiophene- and benzenenitrile-containing symmetric and unsymmetric fulvene ligands. *Organometallics* **2006**, *25* (2), 447−462.

(25) Prabhu, S.; Poulose, E. K. Silver nanoparticles: mechanism of antimicrobial action, synthesis, medical applications, and toxicity effects. *Int. Nano Lett.* **2012**, *2*, 32.